Interface Effects for Cu, CuO, and Cu_2O Deposited on SiO_2 and ZrO_2. XPS Determination of the Valence State of Copper in Cu/SiO_2 and Cu/ZrO_2 Catalysts

J. P. Espinós,* J. Morales, A. Barranco, A. Caballero, J. P. Holgado, and A. R. González-Elipe

Instituto de Ciencia de Materiales de Sevilla, Centro de Investigaciones Científicas, Isla de la Cartuja, Avda, Americo Vespucio s/n, 41092 Sevilla, Spain

Received: December 19, 2001; In Final Form: April 19, 2002

Copper and copper oxides (Cu_2O and CuO) have been deposited by evaporation of copper and subsequent oxidizing treatments, on the surface of flat SiO_2 and ZrO_2 substrates. Large variations of several eVs have been found in the values of the Cu $2p_{3/2}$ binding energy (BE) and Auger parameter (α') of copper as a function of the amount of deposited metallic copper or copper oxides. The magnitude of the changes was also dependent on the type of support upon which the experiment was carried out. These changes have been attributed to modifications in the factors contributing to the initial and final state effects of the process, according to the dispersion degree and the nature of the interactions between the copper oxide moieties and the support. All of these changes can be systematized with the help of chemical state plots. Experiments carried out with real catalysts stress the need of such plots, which summarize the results obtained with the model systems, for a proper characterization of the supported oxide phases in this kind of real materials.

Introduction

Copper oxides are materials widely used because of their importance in the fabrication of supported catalysts,[1−5] in high temperature thermal barriers in metallurgy,[6] and, more recently, in metallization of modern integrated microelectronics components[7] and preparation of high-temperature superconductors.[8] The ability to know the nature of copper interactions with polycrystalline oxides (so-called "real world" oxides) as Al_2O_3, SiO_2, ZrO_2, ZnO_2, MgO, TiO_2, etc., would have immediate impact on processing methods for preparation, activation and regeneration of catalysts, metalization and corrosion inhibition of microcircuits, adhesion and diffusion of thermal barriers or optimization of electrical properties of superconducting thin films.

Usually, the identification of the different oxidation states of copper in bulk oxide samples can be easily carried out by X-ray Photoelectron Spectroscopy (XPS) because different shapes or energy position of the Cu $2p_{3/2}$ photoelectron and Cu L_3VV Auger lines characterize the Cu^+ and Cu^{2+} oxidation states of this element.[9] Thus, the Cu2p spectrum in bulk CuO samples is characterized by large satellite peaks on the high binding energy side of the main photoelectron peaks, which are absent in the spectra for Cu_2O or Cu. On the other hand, although these last two oxidation states show very similar Cu2p spectra, their CuL_3VV Auger lines are energy shifted by ca. 2 eV.

However, the XPS characterization of the oxidation state of transition metal compounds supported as dispersed phases on solid substrates, as nanoparticles, catalysts or very thin films, is not straightforward, and it may be ambiguous because it has been proved that the aggregation state (particle size in nanophases, dispersion degree in catalysts and thickness in thin films) and the interaction of the adsorbate particles with the support may have paramount influences upon the energy position and shape (width, satellite structure,...) of the photoelectron[10−12] and Auger signals,[13,14] as a consequence of changes on the electronic structure of small aggregates. Thus, the modification of spectral features for nanosized metallic particles (v.g. Pt, Rh, Ni, Cu, ...) supported on bulk substrates (other metals, oxides, carbon, ...) has been extensively studied,[10−14] because of its remarkable interest for the characterization by XPS of those metallic particles in technological fields such as ceramics, composites, catalysis, electronics, etc.

In particular, it has been determined[13] that for small particles of Cu, even when supported on a "chemical inert" substrate as graphite, the binding energy of the Cu2p lines increase in about 0.5 eV, while the kinetic energy of the main Auger lines ($CuL_3M_{23}M_{45}$ and $CuL_3M_{45}M_{45}$) diminish in about 2.3 eV. As a result, the Auger parameter α'[15] decreases almost 1.8 eV for small particles sizes, then approaching to the value of Cu_2O bulk compound.[9] Consequently, much work has been devoted to study the formation of several Cu/MO_x interfaces (where MO_x means an oxide), where the support cannot be considered "chemically inert" at all. These studies have been carried out by deposition of metallic copper, under ultrahigh vacuum conditions, on clean and well-defined substrates (in some cases, single-crystal substrates) as Al_2O_3,[16−20] MgO,[21,22] ZnO,[23] Cr_2O_3,[24] or ZrO_2.[25] They have been oriented to know structural and electronic properties of these interfaces, as well as to elucidate the growth mode of the adsorbate[17,18,21−25] or to determine the electronic structure of metallic clusters[13,17,19] and the valence state of copper (Cu^0, Cu^+, or Cu^{2+}),[16,18−23] in submonolayer coverages before any exposition of the interface to reactive gases (CO, H_2, O_2, NO, H_2O, etc.). To these aims, several surface analytical techniques as photoemission spectroscopies (XPS, UPS, AES, and RPES),[16−25] X-ray absorption (EXAFS, XANES),[20] electron spectroscopies (RHEELS and EELS[16,22,23] or ion scattering (LEIS)[17] have been extensively used. Concerning the oxidation state of copper in submonolayer films on oxide supports, which is the main purpose of this paper, in most cases authors have proposed the formation of Cu^+ by reaction of the Cu atoms with the oxide and hydroxide ions in the surface of

* To whom correspondence should be addressed. Telephone: +34-5-4489530. Fax: +34-5-4460665. E-mail: jpespinos@icmse.csic.es.

10.1021/jp014618m CCC: $22.00
Published on Web 06/19/2002

the support, during the initial stages of deposition. When photoemission techniques have been used, the formation of Cu^+ has been inferred from the line shape and/or position of the CuL_3VV signal and the low values obtained for the Auger parameter of Cu. However, it seems clear that this interpretation could be wrong for at least two reasons: first, because similar values for the Auger parameter of Cu have been also obtained for small clusters of metallic copper[13] and, actually, other authors have explained these values at low coverages exclusively by initial and final state screening effects as a function of Cu cluster size,[14,17,24,25] the formation of $Cu^{(+)}$ being consequently excluded. Second, because nobody has previously determined, to our knowledge, these spectral features for small aggregates of Cu_2O or CuO deposited on oxide supports. Actually, despite its technical importance, the study of Metal Oxide/Metal Oxide interfaces by photoemission spectroscopies has deserved few attention and scarce works are available in the literature nowadays. In this context, we have reported in last years on the preparation and electronic characterization of very thin films of TiO_2,[26−29] SnO and SnO_2,[30−32] CoO and Co_3O_4,[33] SiO_2,[34,35] Al_2O_3[36], and MgO[37] supported on polycrystalline metals, oxides, nitrides or graphite, mainly by X-ray photoemission spectroscopies (XPS, XAES, and Resonant Photoemission). Most relevant results from these studies are again the existence of large shifts (of several electronvolts, in comparison with bulk compounds) in the binding energy and/or the Auger parameter of the metallic cations as the particle size of the adsorbate decreases. In addition, for a given adsorbate, energy differences have also been found to depend on the chemical nature of the support and the growth mode. These electronic changes have been explained by initial and final state screening effects as a function of the oxide cluster size and their interaction with the atoms in the support. Recently, a new concept, which has been called "chemical state vector", has been introduced[38] for the characterization of oxide interfaces.

In the present paper, we report about the characterization of the chemical state of copper in the form of Cu°, Cu_2O, and CuO distributed on the surface of two different oxide supports: SiO_2 and ZrO_2. The studied systems consist of increasing amounts of these compounds deposited under ultrahigh vacuum conditions on the surface of flat polycrystalline substrates, from submonolayer coverages up to thick films (bulk deposits).

The actual stoichiometries of the adsorbates have been determined throughout all the experiment by XPS, and controlled by proper treatments with oxygen and plasma of oxygen. In all the cases, large variations in BE and α' of copper have been found.

Finally, the oxidation state of copper in real CuO_x/ZrO_2 and CuO_x/SiO_2 catalysts (powder samples), subjected to several standard reduction and oxidation treatments, has been determined. This study proves that a proper characterization of the chemical state of copper in real catalysts require the comparison of the obtained results with those obtained for model systems.

Experimental Section

Copper was deposited by thermal evaporation from a copper wire wrapped around a tungsten thick wire, which was resistively heated by passing current through it. Power was maintained constant to give reproducible evaporation rates as low as 0.1 monolayer of Cu per minute. Deposition of metallic copper was done in ultrahigh vacuum (base pressure $< 10^{-9}$ mbar, oxygen pressure $< 10^{-10}$ mbar) in the preparation chamber of the XPS spectrometer. For preparation of Cu_2O thin films, submonolayer deposits of copper were exposed to 10^{-2} mbar of oxygen at 298 K for 5 min, and the evaporation-oxidation treatment was repeated as many times as necessary to obtain thicker films of Cu_2O. Finally, preparation of CuO thin films was accomplished by exposure of the submonolayer Cu deposits to a plasma of oxygen, at a pressure of 10^{-2} mbar during 5 min. Oxygen plasma was produced in a tube of quartz, which is directly connected to the pre-chamber of the spectrometer, with a microwave cavity supplied with 75 W from a Microtron 200 generator.

SiO_2 substrates consisted of thin films (∼15 nm thickness) of this compound obtained by thermal oxidation (pure O_2, 873 K, 2 h) of a Si (100) wafer, whereas ZrO_2 substrates consisted of thin films (∼15 nm thickness) of this compound formed electrochemically[39] on the surface of Zr foils (Goodfellow, purity > 99.8%). Before any deposition of copper, both substrates were cleaned, in the pretreatment chamber of the spectrometer, by low energy ion bombardment with O_2^+ (0.5 keV ion kinetic energy), and subsequent treatment with plasma of oxygen, until no traces of carbon were visible by XPS. On these substrates, metallic copper and copper oxides (CuO and Cu_2O) were deposited.

In addition, another experiment was also carried out where Cu was deposited on metallic Zr as a substrate, to obtain reference samples to compare photoemission signals of unoxidized particles of copper with different sizes with those for Cu_2O. In this particular case, a very clean substrate, with no traces of oxygen, was necessary. With this aim in mind, a metallic foil of Zr was subjected to successive Ar^+ sputtering and annealing cycles until no traces of carbon or oxygen could be detected in the spectrum.

Finally, some Cu/ZrO_2 and Cu/SiO_2 powder catalysts have been also investigated after been subjected "in situ" to different reduction/oxidation treatments, with pure H_2 or O_2 gases, in the pre-chamber of the spectrometer. These catalysts were prepared by the incipient wetness impregnation of a ZrO_2 powder ($S_{BET} = 45$ m^2 g^{-1}) or SiO_2 powder ($S_{BET} = 200$ m^2 g^{-1}) with a $Cu(NO_3)_2$ solution, drying at 393 K overnight, and then by being calcined in 3% O_2/He at 573 K for 3 h. The ZrO_2 powder was prepared by forced hydrolysis at 371 K of a 0.2M $ZrOCl_2$ solution for 72 h, and the product obtained was dialyzed to eliminate the chloride ions, and calcined at 773 K for 3 h. On the other hand, SiO_2 was obtained from Degussa (Aerosil 200) and used as received. To have samples with different particle sizes (dispersion degree) of the supported phase (Cu, CuO, or Cu_2O), five samples were prepared on ZrO_2, with nominal loads of 0.3, 3, 6, 9, and 12% of copper, and four samples on SiO_2, with nominal loads of 3, 6, 9, and 12%. For the purposes of obtaining catalysts with copper in clearly defined oxidation states, soft pressed pellets of $1 \times 8 \times 8$ mm^3 were subjected to four consecutive chemical treatments in the preparation chamber of the XPS spectrometer: (a) oxidation with 1 mbar O_2 at 673 K for 30 min, (b) annealing at 673 K in a vacuum (10^{-7} mbar) for 30 min, (c) reduction with 1 mbar H_2 at 523 K for 30 min, and (d) reduction with 1 mbar H_2 at 673 K for 30 min. The dispersion degree of copper in these samples has been estimated by analyzing the evolution of the intensity of the XPS peaks as a function of the metal loading.[40]

XPS spectra were obtained in an ESCALAB 210 spectrometer, consisting of two separate chambers which are independently pumped. Base pressures in the range of 10^{-10} mbar and 10^{-7} mbar are obtained in the analysis and preparation chambers, respectively. Samples were mounted on a mobile Ta sample holder which can be transported on a manipulator rod between both chambers. All experiments reported here were carried out

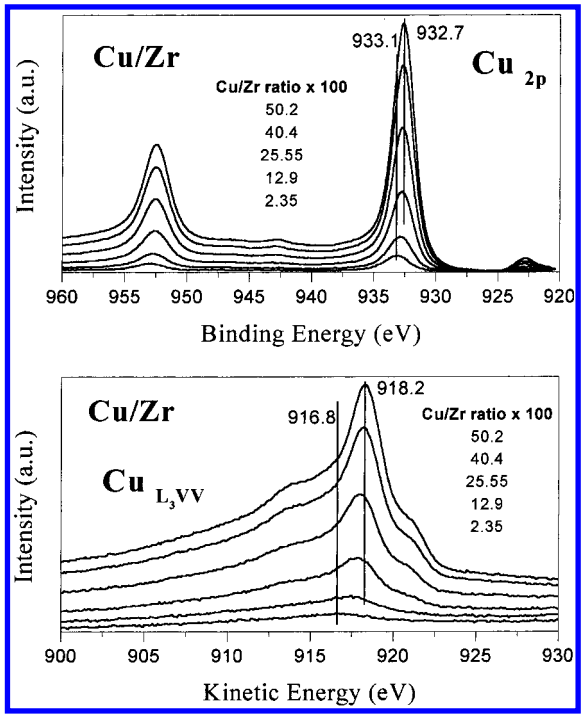

Figure 1. Evolution of Cu2p and Cu L_3VV signals for increasing amounts of Cu° deposited on Zr at room temperature. Coverage has been expressed by the Cu2p/Zr3d intensity ratio determined by XPS. Only a few spectra of the whole series have been depicted for clarity.

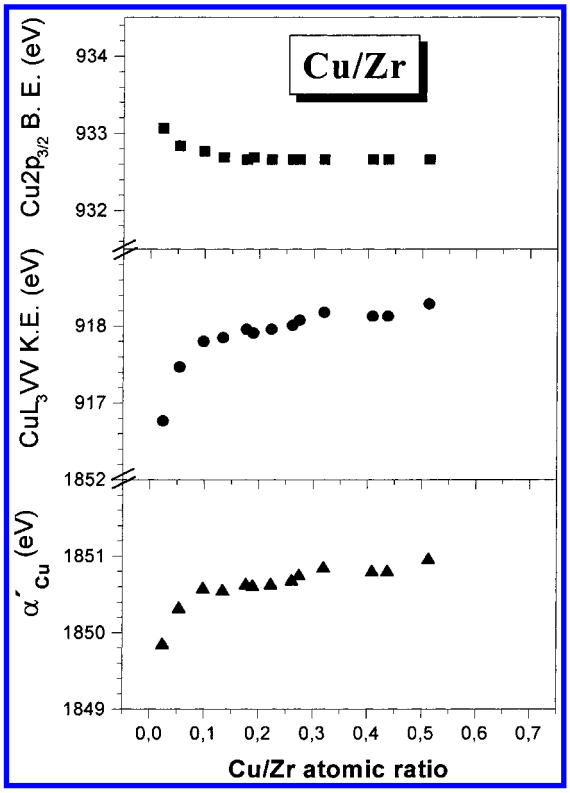

Figure 2. Evolution of the Cu $2p_{3/2}$ BEs, Cu L_3VV KEs and α′ values of copper for increasing amounts of this element deposited on Zr, as a function of the Cu2p/Zr3d ratio determined by XPS. The data correspond to the spectra shown in Figure 1.

with samples at room temperature. A hemispherical electron energy analyzer working in the constant pass energy mode at a value of 50 eV was used. Unmonochromatized Mg Kα radiation was used as excitation source for samples containing SiO_2, whereas Al Kα had to be used for samples containing Zr, because CuL_3VV peak overlaps with Zr3p signal if spectra of theses samples are acquired with Mg Kα. Spectra were energy calibrated by taking Si2p peak at 103.4 eV (BE) or $Zr3d_{5/2}$ peak at 182.2 eV (BE) for SiO_2 or ZrO_2 containing samples, respectively. Experiments carried out on metallic Zr were referenced by $Zr3d_{5/2}$ at 178.9 eV (BE). This seems the best option for studying by XPS insulator oxides which develop considerable charging effects when analyzed by this technique. In this paper, besides BE of photoelectron peaks, we use Auger parameter values. In principle, this parameter is not subjected to charging effects and is a good experimental approach to study insulating materials.

The coverage degree of the different preparations has been expressed as the Cu/M atomic ratio (M: Si, Zr) determined from the areas of the Cu $2p_{3/2}$ and Si2p or Zr3d peaks, modified by the sensitivity factors of these elements, empirically derived from ZrO_2, SiO_2 and Cu single crystals, which are in good agreement with those existing in the literature.[42] As a first approach, a coverage of one equivalent monolayer (ML) can be expected when an atomic ratio Cu/M (M = Si, Zr) = 0.1 is achieved.

Results

Shifts in Cu$2p_{3/2}$ and Cu L_3VV Peak Positions. A series of Cu2p photoelectron and Cu L_3VV Auger spectra for successive evaporations of metallic copper under UHV (pressure $<10^{-9}$ mbar) on the surface of a clean Zr substrate are shown in Figure 1. It is already apparent in the series of Auger spectra that the position of the main peak, at around 916.8 eV KE, shifts to higher kinetic energies, up to 918.2 eV, as the amount of deposited copper increases. After a careful analysis of the Cu2p photoelectron spectra, a shift to lower binding energy values can be also detected, from 933.1 to 932.7 eV. As a summary of these changes, Figure 2 shows the evolution of these peaks as a function of the amount of deposited copper, expressed by the Cu/Zr intensity ratio. Also included in this figure is the evolution of the Auger parameter values.[15] It is clear that the BE decreases and the KE and α′ increase as a function of the amount of deposited copper. It also appears from this figure that most of these changes occur up to coverages at which the Cu/Zr ratio has a value around 0.15 (i.e., slightly above the equivalent monolayer). Finally, it must be noted in Figure 1 that shape changes have not been observed, neither in the Cu2p peak nor in the CuL_3VV, throughout the experiment, suggesting that the copper valence state remains invariable. Energy values found at final deposition are the same as reported for bulk Cu.[42]

Similarly, experiments were carried out for the deposition of Cu_2O and CuO on ZrO_2 and SiO_2 flat substrates. Thus, Figure 3 and Figure 4 show plots of the Cu$2p_{3/2}$ photoelectron and Cu L_3VV Auger spectra for successive depositions of these two compounds on ZrO_2, respectively. Similar spectra were obtained when deposition was done on SiO_2, but they are not shown here. A clear difference in the shapes of the Auger and photoelectron spectra can be observed for the two compounds, being in agreement with those previously reported and discussed in the literature for Cu^+ and Cu^{2+} species.[9] It is also apparent that the position of the Cu$2p_{3/2}$ peak and that of the maximum of the Cu L_3VV spectra shift as a function of the deposited amount of any of the two copper oxides. Although the magnitude of the changes were different, a similar effect was observed during the deposition experiments carried out on SiO_2. In both systems, other changes could be observed in the O1s (and OKLL) spectra that can be explained by the superposition of contributions from the substrates and deposited overlayers, as shown in Figure 5

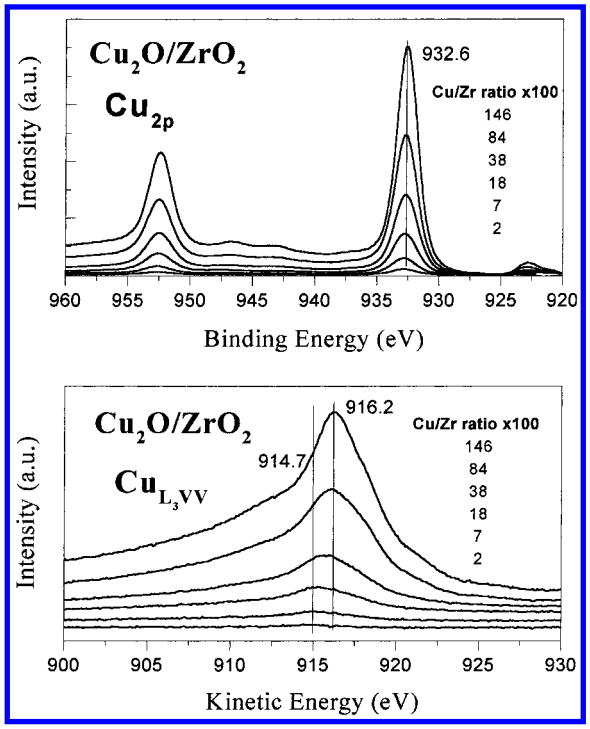

Figure 3. Evolution of Cu2p and Cu L_3VV signals for increasing amounts of Cu_2O deposited on ZrO_2. Coverage has been expressed by the Cu2p/Zr3d intensity ratio determined by XPS. Only a few spectra of the whole series have been depicted for clarity.

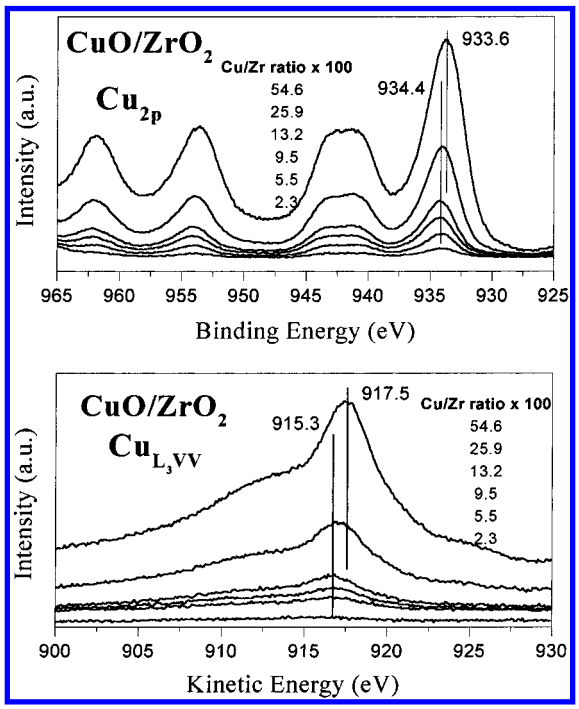

Figure 4. Evolution of Cu2p and Cu L_3VV signals for increasing amounts of CuO deposited on ZrO_2. Coverage has been expressed by the Cu2p/Zr3d intensity ratio determined by XPS. Only a few spectra of the whole series have been depicted for clarity.

for the case of Cu_2O on SiO_2. A proof that the stoichiometries of the two deposited copper oxides were Cu/O = 1 or 2, depending on the preparation conditions, was gained by the analysis of the plots of the O/M atomic ratios (M: Si or Zr) versus the Cu/M atomic ratios in each case. These plots are straight lines whose slopes had a value of 1 or $^1/_2$, depending on the stoichiometry of the deposited copper oxide, as shown in Figure 6. It is interesting to note that for deposition of Cu_2O,

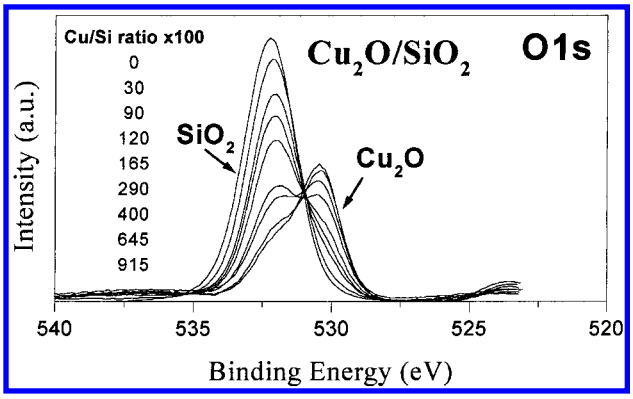

Figure 5. Evolution of O1s signal for increasing amounts of Cu_2O deposited on SiO_2. Coverage has been expressed by the Cu/Si intensity ratio determined by XPS. Only a few spectra of the whole series have been depicted for clarity.

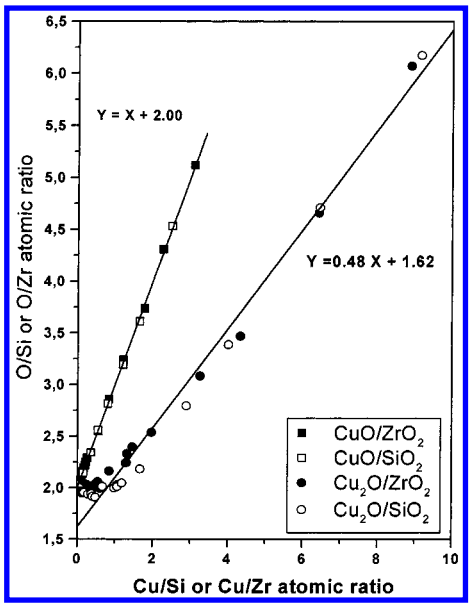

Figure 6. Intensity of the O1s/M (M = Zr3d or Si2p) ratio as a funtion of the coverage of ZrO_2 or SiO_2 with Cu_2O or CuO.

the surface concentration of O does not increase during the first deposition steps. This is likely due to the fact that for very low depositions of copper it may react with small amounts of adsorbed oxygen present on the surface of the oxide supports after their cleaning by O_2^+ bombardment. Of course, this process will not yield any increase in the overall amount of oxygen in the sample and the O/M (M: Si or Zr) XPS ratio remains constant during this initial deposition period. The evolution of the different electronic parameters of copper (i.e., BE, KE, and α') with the amount of the deposited oxides can be seen in Figures 7 and 8. As in the previously described experiment for the metallic copper (cf. Figure 2), most of the changes in the value of these parameters occur for relatively low coverages up to Cu/M ratios of 0.2, although in some cases higher coverages are necessary to reach the values reported for bulk copper oxides.[9]

A summary of the magnitude of the changes between the values of the lower and higher coverage layers prepared are presented in Table 1. These differences should account for the total change of these parameters for the smallest moieties of deposited copper in their different chemical forms and the corresponding bulk compounds. For comparison, some data from the literature corresponding to Cu evaporated on carbon (highly oriented pyrolitic graphite) are also included.[13]

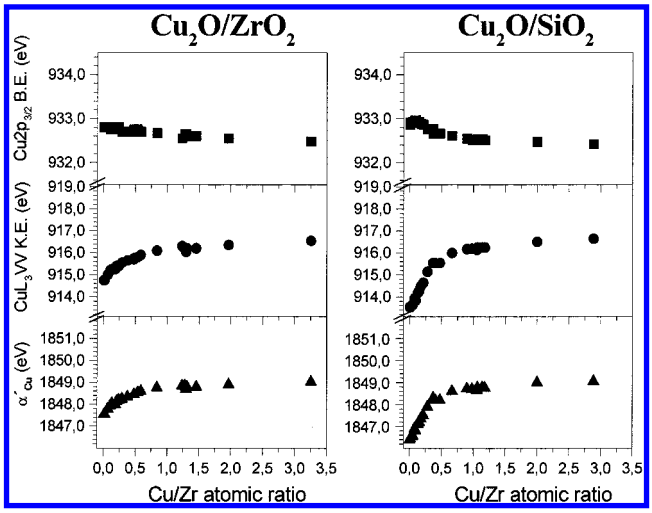

Figure 7. Evolution Cu $2p_{3/2}$ BEs, Cu L_3VV KEs and α' values (eV) of copper for increasing amounts of Cu_2O deposited on ZrO_2 (left panel) and SiO_2 (right panel).

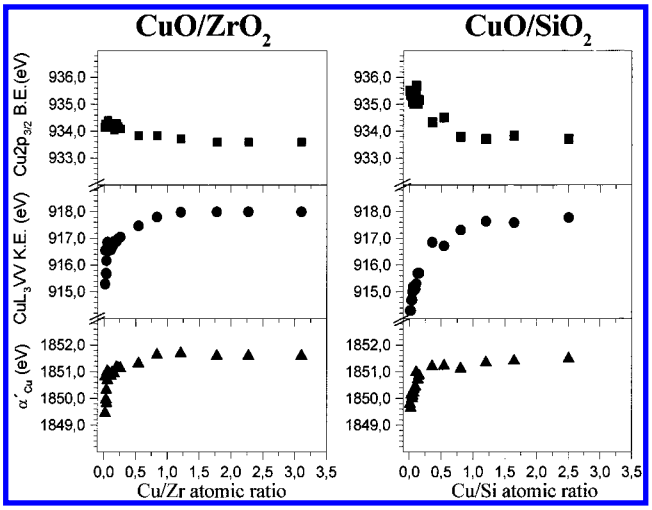

Figure 8. Evolution of the Cu $2p_{3/2}$ BEs, Cu L_3VV KEs and α' values (eV) of copper for increasing amounts of CuO deposited on ZrO_2 (left panel) and SiO_2 (right panel).

Chemical State Plots for Copper Oxides Deposited on Oxide Substrates. XPS characterization of chemical states of an element in different compounds is usually carried out by comparing their BE and α' values in a Wagner plot.[15,41] In previous papers, we have used this type of graph to summarize in a single plot all the changes occurring when a metal oxide thin film is deposited on another metal oxide support,[28,32,36,38] even when there is no change in the chemical state of the elements. The reported changes have been attributed to specific bonding interactions appearing at the interface between the two oxide phases and/or to modifications in the polarization properties of the two materials brought into contact.[27,30,31] For the set of experiments carried out here a similar plot is presented in Figure 9. In this Wagner plot, a series of points rather than a single point characterize each chemical state of copper. We will refer to this array of points as "chemical state lines". The data in Figure 9 define three "chemical state lines", for metallic copper, Cu_2O, and CuO, respectively. In each case, the chemical state line includes the points corresponding to the experiments on the two substrates (i.e., SiO_2 and ZrO_2). The arrows indicate how the amounts of deposited copper or copper oxides increase during the experiments. It is interesting to note that for metallic copper and Cu_2O, changes for α' are larger than for BE, whereas for CuO both parameters, α' and BE, change significantly with the amount of deposited copper.

Applications: Characterization of Chemical States of Copper in Real Systems. Characterization of the chemical state of an element by XPS has been traditionally carried out by comparing their BE and α' values with those of reference compounds. The results described above and other previously published by our laboratory[26−38] show that this can be a misleading procedure when dealing with well dispersed phases on substrates. In this particular case, very large changes in these two parameters can be found as a function of the dispersion degree of the supported phase. Obviously, this is the situation when dealing with catalyst systems or very thin films.

In the following paragraphs, some results for a series of Cu/ZrO_2 and Cu/SiO_2 catalyst systems are presented within the frame of the Wagner plot of copper. As described in the Experimental Section, these catalysts have different copper loadings and were subjected to different activation treatments under oxidation (O_2, 673 K) and reduction (vacuum at 673 K, H_2 at 523 K or H_2 at 673 K) conditions. An analysis of the dispersion degree of cooper in these samples show that it decreases as the amount of cooper in the samples increases. This is clearly illustrated by the diagram in Figure 10, showing the evolution of the relative intensities of the Cu_{2p} peaks as a function of the metal loading. The reported curves show an initial increase in intensity followed by a constant value of the Cu/M (M = Si, Zr) ratio as the loading increases above 6%. In the figure, the dotted line indicates the evolution of intensity that should have been expected for a complete dispersion of the copper.[40] The evolution in Figure 10 corresponds to the original samples before any treatment. A similar behavior was also found for these samples after the reduction and oxidation treatments specified above, thus indicating that a similar evolution occurs for the size of the copper aggregates in these samples (data not shown). These representations confirm that the size of the copper aggregates change with the amount of copper in the sample and, in principle, enable to perform an analysis of BE and α' values similar to that carried out with the evaporated systems in previous sections.

In this sense, Figures 11 and 12 show the values of the electronic parameters for copper in these samples in Wagner plots, where ideal "chemical state lines" corresponding to the Cu^0, Cu_2O and CuO states of this element are also plotted according to the experimental values depicted in Figure 9.

Several issues deserve to be noted in these two last figures. First, as expected from the previous results with model systems, large differences in the electronic parameters were found for the powder samples, depending on the dispersion degree of the supported phase, being in some particular cases quite far from the values reported for bulk compounds. It seems clear to us, from data in Figure 9, that these "anomalous" electronic parameters do not indicate the formation of ternary compounds (i.e., copper silicates, ...) at all, but they reflect the different dispersion degree of the supported phase. Second, from the position of the experimental points in relation with the "chemical state lines" in these two diagrams, it is clear the attribution of the oxidation states of copper in each case, a result which is particularly interesting for a rapid and precise identification of Cu(0) or Cu(I) oxidation states in samples with a high dispersion degree.

Third, a comparison of the data in Figures 11 and 12 suggests that ZrO_2 support strongly stabilizes the Cu(I) state because these species can be obtained just by annealing under ultrahigh vacuum, while a reduction treatment more severe (H_2 at 523

TABLE 1: Summary of Spectroscopic and Calculated Electron Parameters Obtained for the Indicated Systems (all data in eV)

	$Cu2p_{3/2}$ binding energy (eV)			**CuL_3VV** kinetic energy (eV)			α'_{Cu} auger parameter (eV)				
sample	bulk	dispersed	ΔBE	bulk	dispersed	ΔKE	bulk	dispersed	$\Delta\alpha_{Cu}$	**ΔRE** (eV)	$\Delta\epsilon$ (eV)
Cu/Zr	932.7	933.1	−0.4	918.6_5	916.8	1.8_5	1851.3	1849.9	1.4_5	0.7	0.3
Cu/C[a])	932.7	933.2	−0.5	918.6_5	916.3_5	2.3	1851.3	1849.5	1.8	0.9	0.4
CuO/ZrO_2	933.6	934.4	−0.8	918.0	915.2_5	2.7_5	1851.6_5	1849.6_5	2.0	1.0	0.2
CuO/SiO_2	933.6	935.4	−1.8	918.0	914.4	3.6	1851.6_5	1849.8	1.8_5	0.9	−0.9
Cu_2O/ZrO_2	932.5	932.8	−0.3	916.6_5	914.7_5	1.9	1849.3	1847.6	1.7	0.8_5	0.5_5
Cu_2O/SiO_2	932.5	932.8_5	-0.3_5	916.6_5	913.6	3.0_5	1849.3	1846.4_5	2.8_5	1.4	0.8

[a] Data from literature (ref 13). [b] Estimated differences in extra-atomic relaxation energy (ref 43) in the final state ($\Delta RE = 1/2\Delta\alpha'$). [c] Estimated differences in initial state energies (ref 43) calculated according to $\Delta\epsilon = \Delta BE + \Delta RE$.

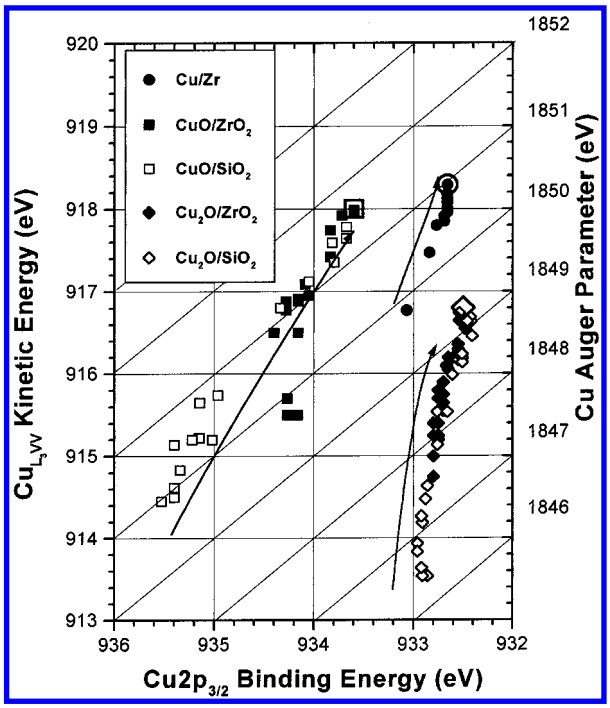

Figure 9. Wagner plots for Cu°, Cu_2O, and CuO for increasing amounts of these compounds deposited on the surface of different flat substrates as indicated. The arrows show the tendency of evolution with the amount of deposited material. The big symbols refer to the values found for the bulk materials.

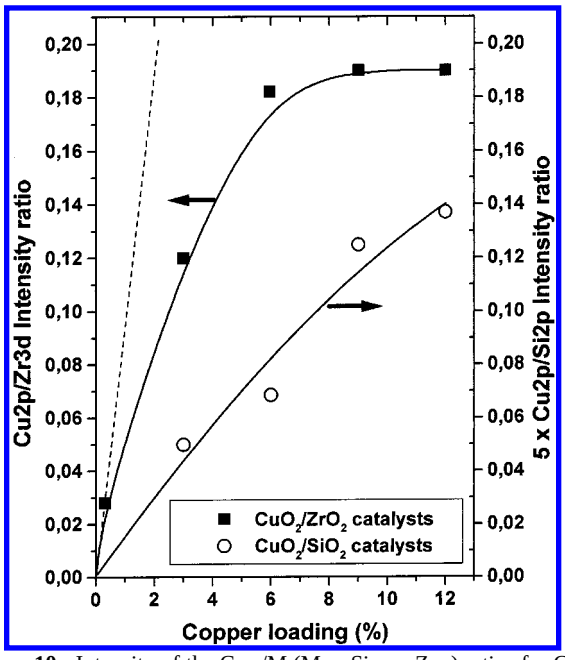

Figure 10. Intensity of the Cu_{2p}/M (M = Si_{2p} or Zr_{3d}) ratios for CuO/SiO_2 and CuO/ZrO_2 catalysts as a function of copper contents.

K) is necessary for the case of SiO_2 supported samples. Actually, data regarding Cu/SiO_2 samples heated under UHV are not included in Figure 12 because mixtures of Cu(II) and Cu(I) are always found. Note also that well dispersed Cu(I) species (on both substrates, samples with lower Cu content) are not easily reduced to metal.

Finally, the use of the Wagner plot provides an additional information regarding the dispersion degree of copper in real catalysts. Thus, the agglomeration of points in the same position of the plot in Figure 11 found for the set of Cu/ZrO_2 catalysts (with different Cu loadings) after the oxidative treatment, indicates that the particle size of copper oxide should be rather similar and very high in all the samples considered here, whereas for the Cu/SiO_2 set only the sample with lower content in copper (3%) would be originally well dispersed (see Figure 12). Moreover, it seems clear that mild reduction treatments (vacuum at 673 K for Cu/ZrO_2 samples or H_2 at 523 K for Cu/SiO_2 ones) leads to well dispersed Cu_2O particles, especially for the zirconia supported samples. In both systems, reduction to metallic copper usually takes place with an increase in the particle sizes.

Discussion

The observation of the chemical state plot in Figure 9 clearly indicates that a large set of BE and α′ values should be expected for copper and copper oxide phases when they are dispersed on the surface of other substrates. For particles of metallic copper and other metals, changes in the BE of photoelectron peak and in the Auger parameter have been reported since long ago. These changes have been attributed to final and initial state effects and correlated with the size of the deposited metal particles.[10−14] Several reasons have been invoked: changes in the average coordination number of the particle atoms owing to a high surface-to-volume ratio, decrease of the electron density of the particles in respect to the bulk metal, narrowing of the valence band, alloying and/or chemical interactions with the substrate, etc. In the experiment carried out here with metallic copper deposited on zirconium metal, the changes observed in the BE and α′ parameters with the amount of deposited copper should be originated by one or more of those reasons (cf. Figures 1, 2, 9 and Table 1).

Similar changes on the electronic parameters have been also reported for small oxide particles or layers deposited on substrates of other oxide materials. Thus, we have found large changes in BE and α′ for a relatively large series of oxides including TiO_2,[26−28] SiO_2,[34,35] SnO,[30] SnO_2,[31] CoO,[33] and Al_2O_3[36] supported on different substrates. The experiments carried out here for Cu_2O and CuO show that in these cases significant changes in electronic parameters can be also found depending on the dispersion degree of the supported phase and on the type of oxide acting as substrate. Assuming that the dispersion degree of the deposited phases decreases with the amount of deposited material (i.e., according to the Cu/M ratio), we have found that BE decreases and α′ increases when going

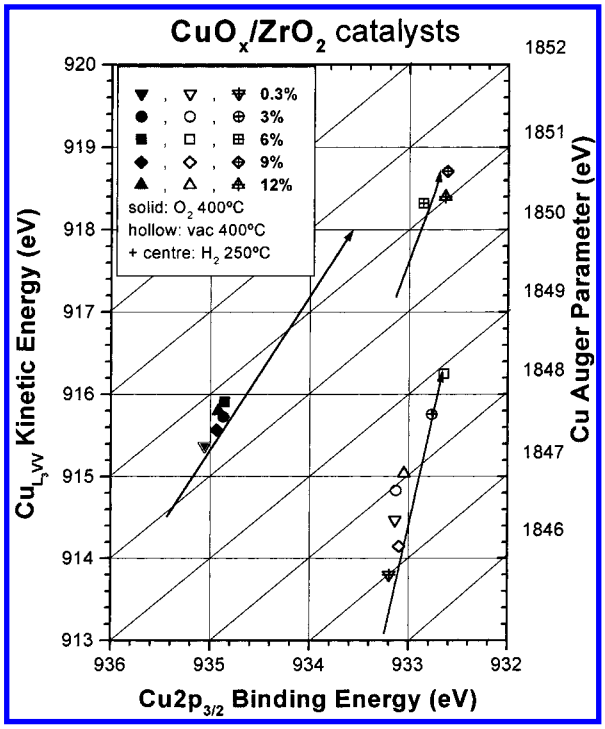

Figure 11. Wagner plot for copper in a series of Cu/ZrO_2 catalysts in comparison with the "chemical state lines" characterizing Cu°, Cu_2O, and CuO dispersed on the surface of SiO_2 and ZrO_2.

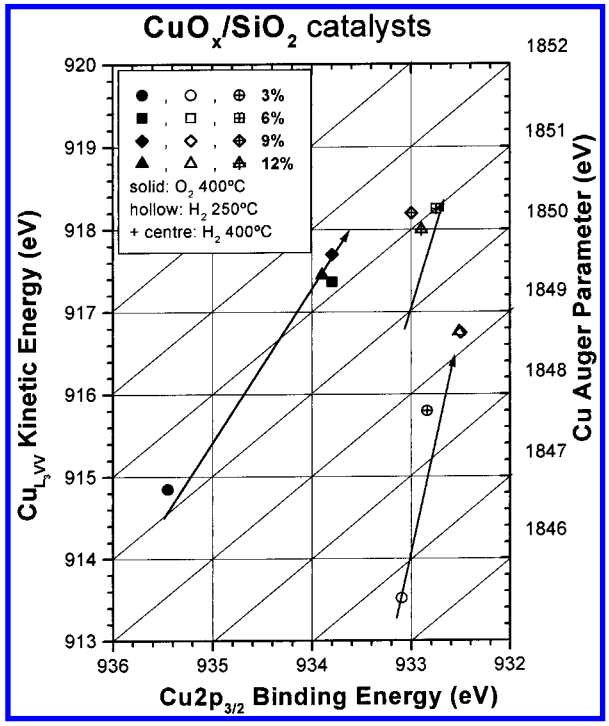

Figure 12. Wagner plot for copper in a series of Cu/SiO_2 catalysts in comparison with the "chemical state lines" characterizing Cu°, Cu_2O, and CuO dispersed on the surface of SiO_2 and ZrO_2.

from a dispersed to an agglomerated state. Total changes in ΔBE and in $\Delta\alpha'$ are reported in Table 1. Also, in this table we have reported the changes in relaxation energy of photoholes (i.e., ΔRE) and in the initial state energy of the system (i.e., $\Delta\epsilon$), calculated according to the appropriate relationships.[43] The reported values show that both initial and final state effects are contributing to the changes in the electronic parameters (BEs and α'). A very thorough analysis of these variations between the very dispersed phases and the bulk materials can be done by comparing these changes with quantum mechanical of the Cu−O−M (M: Si, Zr) bond structure at the interface.[27,35] However, this theoretical analysis is outside the scope of this paper aiming at a phenomenological description of interface effects. Just on a semiquantitative basis, data in Table 1 reveal that, for both Cu_2O and CuO, change in relaxation energy is higher when the substrate is SiO_2 than ZrO_2, probably pointing to the difference in the overall polarizability of these two substrates.[35] By contrast, the differences in the initial state energy do not follow a common scheme for the two substrates, thus suggesting to a complex variation of initial state effects (e.g., distribution of electron densities at the cation, Madelung potentials, etc.).

In previous papers dealing with other supported metal oxides, several reasons have been discussed as responsible for the observed changes. These can be summarized as follows:

(a) One possible reason could be a change in the coordination number around the deposited element for low coverages in the monolayer range. This different coordination provokes a change in the Madelung potential around the photoemitting element and a subsequent variation of the BE and α' values. We found this situation for Al_2O_3 supported on SiO_2.[36]

(b) The observed changes could also be caused by bonding interactions at the interface. The formation of M−O−M′ cross linking bonds at the interface, where the bridging oxide ions should have different electronic characteristics than in the bulk oxides, was invoked as the reason for such contribution. The influence of such an effect was estimated by means of quantum mechanical calculations with cluster models for TiO_2[27] and SnO_2[31] deposited on SiO_2, and for SiO_2 deposited on TiO_2 and Al_2O_3.[35]

(c) Differences in the polarization properties of the two oxides put in contact (i.e., value of their dielectric constants) could also cause the observed changes. This contribution is not restricted to the first monolayer, and it could be estimated as a function of the thickness of the deposited layer by a model based on the Kirwood's formulas for polarization of a dielectric medium.[44]

In addition to these factors, another reason can be invoked to account for changes in the photoelectronic parameters for CuO. It has been recently shown by high-resolution XPS experiments of Cu^{2+} compounds that the Cu $2p_{3/2}$ peak is characterized by a complex shape that changes with the linking arrangement of the Cu^{2+} ions within the lattice.[45] Thus, isolated Cu^{2+} ions surrounded by other metal cations as second neighbors depict a complete different peak shape that Cu^{2+} ions arranged in rows or planes of $Cu^{2+}-O^{=}$ octahedra. These changes are due to modifications in the screening mechanism of photo holes depending on the structure of the compound. By conventional XPS analysis of copper oxide, such changes in peak shapes might lead to shifts in the BE position of the $Cu2p_{3/2}$ peak and changes in the distance and relative intensities between the main and satellite peaks of that line. Indeed, some small changes in these parameters have been found depending on the particle size[46] in a recently reported paper on CuO particles of different sizes, although we could not see any significant change in the peak shapes for the experiments on CuO presented above.

In summary, the observed changes in electronic parameters found in our experiments for supported CuO and Cu_2O could be due to one or more of the above-mentioned factors. Unfortunately, it is not possible to discuss these factors on a quantitative basis at present stage because no structural information about the state of copper at low and high coverages is

available (i.e., coordination state, arrangement of Cu^{2+} cations). These pieces of information and a quantum mechanical description of the Cu−O−M bond at the interface in terms of covalence, density of charge distribution, etc., would be necessary to completely account for the observed changes. Just on a qualitative basis, it could be argued that the covalency of such a Cu−O−M bond should be higher when depositing the copper oxide on SiO_2 than on ZrO_2, a factor that likely should contribute to shift the BE of Cu to higher values when dispersed on SiO_2 than on ZrO_2, as it has been experimentally found.

Our results on Cu/SiO_2 and Cu/ZrO_2 catalyst agree very well with those previously reported by Grünert et al.,[47] who found high XPS binding energies and low Auger kinetic energies for Cu, CuO and Cu_2O small clusters dispersed in copper/ZSM-5 catalysts. These authors report decreases of ~3.7 eV in the KE of the CuL_3VV Auger line and ~2.2 eV in the Auger parameter for well dispersed CuO and Cu_2O species, likely located in the channels of the zeolite, with respect to bulk copper oxides, respectively. In addition, when these catalysts are reduced with H_2 at 523 K, they observed by EXAFS that very small metallic Cu particles are formed (average particle diameter ≈ 1 nm), and a change in the Auger parameter of −4 eV is obtained with respect to bulk Cu. They suggest that these changes reflect the decrease of the extra atomic relaxation energy term due to the high dispersion of the copper species and also the specific coordination of copper ions in zeolite framework.

Conclusions

The values of BE and α′ of supported metal oxides of copper are very sensitive to the dispersion degree of the supported phase and to the type of support on which they are deposited. Large differences in these two parameters have been found for CuO and Cu_2O deposited on SiO_2 and ZrO_2 according to the amount of deposited oxides. Experimental procedures have been developed to get these two copper oxide phases from the evaporation of metallic copper on these two substrates. The observed changes depend on the nature of the support and on the dispersion degree of the dispersed phase and occur mainly for low coverage degrees of the deposited material, equivalent to a few monolayers.

The plot of the observed shifts in a Wagner diagram may be a practical way of dealing with these differences. To get an idea of the expected magnitude of the changes, it would be desirable to have available plots for several $Cu_xO/M'O$ systems. Here, data for SiO_2 and ZrO_2 used as substrates have been provided. The data cover a large set of experimental variation, as expected from the different ionicity and dielectric properties of these two oxide materials.

Characterization of supported metal oxide catalysts and other dispersed systems is very easy if such Wagner plots are available. A comparison of the BE and α′ parameters of the supported phases with the data in the plots, obtained for model systems, provides an immediate identification of the chemical state of the dispersed phases. As an additional bonus, some qualitative information about the dispersion degree of the supported phase can be obtained from such a comparison.

Finally, it must be remarked that identification of chemical states of elements pertaining to dispersed oxide phases can be misleading if only BE values are taken into consideration. The previous results and other obtained for different oxide/oxide systems show that, for the same oxidation state, BE and α′ can change depending on the dispersion degree. Depending on the element, a proper evaluation requires the comparison of the values of these two parameters within Wagner plots, which define different "chemical state lines" of the element. These plots should be constructed for each oxidation state of the element and different support materials. At present, besides the plot for copper oxides presented above, similar diagrams are available for TiO_2, SiO_2, Al_2O_3, SnO, and SnO_2 oxides supported on different oxide materials.[38]

Acknowledgment. We thank the Spanish Ministry of Science and Technology for financial support (Project No. 1FD97-0692-C02-01).

References and Notes

(1) Schilke, T. C; Fisher, I. A.; Bell, A. T. *J. Catal.* **1999**, *184*, 144.
(2) Okamoto, Y.; Kubota, T.; Gotoh, H.; Ohto, Y.; Aritani, H.; Tanaka, T.; Yoshida, S.; *J. Chem. Soc. Faraday Trans.* **1998**, *94*, 3743.
(3) Matsuoka, M.; Ju, W. S.; Takahashi, K.; Yamashita, H.; Anpo, M. *J. Phys. Chem. B* **2000**, *104*, 4911.
(4) Yatsu, T.; Nishimura, H.; Fujitani, T.; Nakamura, J. *J. Catal.* **2000**, *191*, 423.
(5) Yokomichi, Y.; Yamabe, T.; Kakumoto, T.; Okada, O.; Ishikawa, H.; Nakamura, Y.; Kimura, H.; Yasuda, I. *Appl. Catal. B-Enviromental* **2000**, *28*, 1,
(6) Stott, F. H. *Rep. Prog. Phys.* **1987**, *50*, 861.
(7) National Technology Road map for Semiconductors, Semiconductor Industry Association, San José, CA, 1997.
(8) Bednorz, J. G.; Müller, K. A. *Z. Phys. B*, **1986**, *64*, 189.
(9) Fleisch, T. H.; Mains, G. J. *Appl. Surface Sci.* **1982**, *10*, 51.
(10) Mason, M. G. *Phys. Rev. B* **1983**, *27*, 748.
(11) Egelhoff, W. F. Jr. *Phys. Rev. B* **1984**, *30*, 1052.
(12) González-Elipe, A. R.; Munuera, G.; Espinós, J. P. *Surf. Interface Anal.* **1990**, *16*, 375.
(13) Jirka, I. *Surf. Sci.* **1990**, *232*, 307.
(14) Moretti, G.; Porta P. *Surf. Sci.* **1993**, *287/288*, 1076, and references therein.
(15) The modified Auger parameter α′ is defined as α′ = Ek(jkl)+Eb(i), where Ek is the kinetic energy of the Auger transition jkl and Eb(i) is the binding energy of the photoelectron emitted from atomic level i. This parameter is independent of charge referencing mistakes, and it was introduced by Wagner, C. D. *Faraday Discuss. Chem. Soc.* **1975**, *60*, 291.
(16) Guo, Q.; Moller, P. J. *Surf. Sci.* **1991**, *244*, 228.
(17) Wu, Y.; Garfunkel, E.; Madey, T. E. *J. Vac. Sci. Technol. A* **1996**, *14*, 1662.
(18) Kelber, J. A.; Niu, C; Shepherd, K; Jennison, D. R.; Bogicevic, A. *Surf. Sci.* **2000**, *446*, 76.
(19) Vijayakrishnan, V.; Rao, N. C. R. *Surf. Sci. Lett.* **1991**, *255*, L516.
(20) Gota, S.; Gautier, M.; Douillard, L.; Thromat, N.; Duraud, J. P.; Fèvre, P. L. *Surf. Sci.* **1995**, *323*, 163.
(21) Alstrup, I.; Moller, P. J. *Appl. Surf. Sci.* **1988**, *33/34*, 143.
(22) Conard, T.; Ghijsen, J.; Vohs, J. M.; Thiry, P. A.; Caudano, R.; Johnson, R. L. *Surf. Sci.* **1992**, *265*, 31
(23) Moller, P. J.; Nerlov, J. *Surf. Sci.* **1994**, *307−309*, 591.
(24) Di Castro, V.; Furlani, C.; Polzonetti, G.; Cozza, C. *J. Electron Spectrosc. Relat. Phenom.* **1979**, *17*, 299.
(25) Sotiropoulou, D.; Ladas, S. *Surf. Sci.* **2000**, *452*, 58.
(26) Lassaletta, G.; Fernández, A.; Espinós, J. P.; González-Elipe, A. R. *J. Phys. Chem.* **1995**, *99*, 1484.
(27) Mejias, J. A.; Jiménez, V. M.; Lassaletta, G.; Fernández, A.; Espinós, J. P.; González-Elipe, A. R. *J. Phys. Chem.* **1996**, *100*, 16 255.
(28) Jiménez, V. M.; Lassaletta, G.; Fernández, A.; Espinós, J. P.; González-Elipe, A. R. *Surf. Interface Anal.* **1997**, *25*, 292.
(29) Espinós, J. P.; Lassaletta, G.; Caballero, A.; Fernández, A.; González-Elipe, A. R.; Stampfl, A.; Morant, C.; Sanz, J. M. *Langmuir* **1998**, *14*, 4908.
(30) Jiménez, V. M.; Fernández, A.; Espinós, J. P.; González-Elipe, A. R. *Surf. Sci.* **1996**, *350*, 123.
(31) Jiménez, V. M.; Mejias, J. A.; Espinós, J. P.; González-Elipe, A. R. *Surf. Sci.* **1996**, *366*, 545.
(32) Jiménez, V. M.; Espinós, J. P.; González-Elipe, A. R. *Surf. Sci.* **1996**, *366*, 556.
(33) Jiménez, V. M.; Espinós, J. P.; González-Elipe, A. R. *Surf. Interface Anal.* **1998**, *26*, 62.
(34) Espinós, J. P.; Stabel, A.; González-Elipe, A. R. *Surf. Sci.* **1998**, *325*, 326.
(35) Barranco, A.; Yubero, F.; Mejías, J.A.; Espinós, J. P.; González-Elipe, A. R. *Surf. Sci.* **2001**, *482−485*, 680.
(36) Reiche, R.; Yubero, F.; Espinós, J. P.; González-Elipe, A. R. *Surf. Sci.* **2000**, *457*, 199.

(37) Holgado, J. P.; Barranco, A.; Yubero, F.; Espinós, J. P.; González-Elipe, A. R. *Surf. Sci.* **2001**, *482*−*485*, 1325.
(38) Barranco, A.; Yubero, F.; Espinós, J. P.; González-Elipe, A. R. *Surf. Interface Anal.* **2001**, *31*, 761.
(39) Sanz, J. M. Thesis, University of Stuttgart, **1982**.
(40) Kerkhof, F. P. J. M.; Moulijn, J. A. *J. Phys. Chem.* **1979**, *83*, 1612.
(41) Wagner C. D.; Davis, L. E.; Zeller, M. V.; Taylor, J. A.; Raymond R. H.; Gale, L. E. *Surf. Interface Anal.* **1979**, *1*, 26.
(42) American Society for Testing and Materials, E 902−88, *Surf. Interface Anal.* **1991**, *17*, 889.
(43) Moretti, G. *J. Electron. Spectrosc. Relat. Phenom.* **1998**, *95*, 95.
(44) Kirwood, G. J. *J. Chem. Phys.* **1934**, *2*, 351.
(45) Böske, T.; Maiti, K.; Knauff, O.; Ruck, K.; Golden, M. S.; Krabbes, G.; Fink, J.; Osafune, T.; Motoyama, N.; Eisaki, H.; Uchida, S. *Phys. Rev. B*, **1998**, *57*, 138.
(46) Chusuei, C. C.; Brookshier, M. A.; Goodman, D. W. *Langmuir* **1999**, *15*, 2806.
(47) Grünert, W.; Hayes, N. W.; Joyner, R.W.; Shpiro, E. S.; Rafiq H.; Siddiqui, M.; Baeva, G. N. *J. Phys. Chem.* **1994**, *98*, 10 832.